Quantitative assessment of osteomyelitis in the mandible using digital imaging

デジタル画像を用いた下顎骨骨髄炎の定量評価

日本大学大学院松戸歯学研究科

放射線学

廣畠　彰哉

（指導：　金田　隆　教授）

本論文は、

1. Quantitative and qualitative assessment of osteomyelitis of the mandible for prognosis prediction using diffusion-weighted magnetic resonance imaging

   Journal of Digital Dentistry (in press)

2. Quantitative assessment of mandibular bone marrow using computed tomography texture analysis for detect stage 0 medication-related osteonecrosis of the jaw

   European Journal of Radiology（第 145 巻　令和 3 年 12 月発行）

をまとめたものである。

1. Abstract

Purposes:

The purposes of this study were 1) to assess the imaging findings of osteomyelitis of the mandible using diffusion-weighted magnetic resonance imaging (DWI) and predict the prognosis, and 2) to quantitatively assess the mandibular bone marrow using texture analysis to detect stage 0 medication-related osteonecrosis of the jaw (MRONJ) from computed tomography (CT) images.

Materials and Methods:

1) This study included 61 patients with osteomyelitis of the mandible (13 men and 48 women, mean age: 68.8 years) who underwent magnetic resonance imaging (MRI). The apparent diffusion coefficient (ADC) value of the mandibular bone marrow was measured on the ADC map. Statistical analysis was performed using Welch's t-test, dividing the cases into two groups: a group in which osteomyelitis symptoms persisted for 4 weeks or more and a group in which symptoms improved in less than 4 weeks. Receiver operating characteristic (ROC) analysis was performed to determine the ability of ADC value to predict the prognosis of mandibular osteomyelitis.

2) This retrospective study included 25 patients with stage 0 MRONJ who had a history of treatment with bisphosphonates and underwent CT and magnetic MRI. The mandibular bone marrow with abnormal signals (T1-weighted imaging: low, T2-weighted

imaging: low or high, short-tau inversion recovery: high) on MRI, and no qualitative characteristic CT and oral findings indicative of osteonecrosis (exposed bone, sequestrum, periosteal reaction, and osteolysis) was identified as 0 MRONJ. Texture features of the bone marrow of the mandible with MRONJ and the contralateral, normal mandibular bone marrow were extracted using an open-access software, namely, LIFEx. The volumes of interest (VOIs) were manually placed on CT images by tracing the bilateral mandibular bone marrow regions, excluding the teeth, mandibular canal, and cortical bone. Thirty-seven texture features were extracted from each VOI.

Results:

1) The mean ADC value of the mandibular bone marrow was 1.377×10^{-3} mm^2/s in the symptom-persisted group and 1.198×10^{-3} mm^2/s in the symptom-improved group. A cutoff value of $>1.303 \times 10^{-3}$ mm^2/s was obtained from the ROC curve using the Youden index.

2) Six gray-level run length matrix features and four gray-level zone length matrix features exhibited significant differences between mandibular bone marrow with and without MRONJ.

Conclusions:

This study revealed 1) the ADC values of the mandibular bone marrow in persisted osteomyelitis and that in improved osteomyelitis and 2) CT texture analysis revealed the quantitative differences between the bone marrow of the mandible with stage 0 MRONJ and the contralateral, normal mandibular bone marrow. These results suggested that quantitative assessment of osteomyelitis in the mandible using digital imaging could be very useful information in clinical situations.

2. Introduction

Osteomyelitis of the jaw is an inflammatory disease of the bone marrow of the jaw bone secondary to an abscessed tooth or postoperative infection[1-4]. The inflammation of osteomyelitis of the jaw can spread over a wide area of the jawbone, including the cortex, cancellous bone, and periosteum. Osteomyelitis is more common in the mandible than in the maxilla because the vascular supply to the mandible is less[5]. Clinical symptoms of osteomyelitis of the mandible include fever, malaise, swelling, local redness, and pain around the soft tissue, and if the condition becomes severe, surgery may be required. Therefore, predicting the prognosis of osteomyelitis of the mandible from imaging is a challenge for clinicians.

Magnetic resonance imaging (MRI) can detect inflammatory diseases non-invasively and is useful in the evaluation of osteomyelitis of the mandible[6-8]. In particular, diffusion-weighted magnetic resonance imaging (DWI) provides information about the Brownian motion of water and has been applied in recent years to a wide variety of lesions, including tumors and cysts[9-13]. DWI is able to quantitatively evaluate images using apparent diffusion coefficient (ADC) values. Non-invasive imaging techniques play an important role in the early diagnosis and follow-up of skeletal inflammatory conditions.

Medication-related osteonecrosis of the jaw (MRONJ) is one of the serious

complications of treatment with bisphosphonates or antiangiogenic inhibitors. The special

committee of the American Association of Oral and Maxillofacial Surgeons recommends

changing the nomenclature of bisphosphonate-related osteonecrosis of the jaw (BRONJ)

to MRONJ[14]. However, it has been reported that imaging findings differ between BRONJ

and antiangiogenic inhibitor-related osteonecrosis of the jaw[15]. Therefore, when

considering imaging findings of osteonecrosis of the jaw, it is appropriate to consider

BRONJ and antiangiogenic inhibitor-related osteonecrosis of the jaw separately. MRONJ

has four stages (0–3). Computed tomography (CT) is often the initial imaging technique

used for confirming the presence or absence of qualitative findings such as exposed bone,

sequestrum, periosteal reaction, and osteolysis, and identifying the causative

inflammation in a suspected case of osteomyelitis[16-19]. Recently, the usefulness of

radiomics, which is a process that analyzes lesions using quantitative features extracted

from medical images, has been highlighted[20,21]. Texture analysis can quantify the texture

in the volume of interest (VOI) of an image by identifying the spatial pattern of pixels,

and is a common technique used in radiomics to quantify images[22]. In recent years,

Texture analysis has been used for various diseases and tissues throughout the body to

quantitatively assess the subtle pathological changes in medical images that were difficult

to identify by conventional diagnostic imaging with the human eye[23-25]. However, there

8

are few studies that to assess the prognosis of mandibular osteomyelitis, and stage 0

MRONJ quantitative features using digital imaging.

The purposes of this study were 1) to assess the imaging findings of osteomyelitis of

the mandible using DWI and predict the prognosis, and 2) to quantitatively assess the

mandibular bone marrow using texture analysis to detect stage 0 MRONJ from CT images.

3. Materials and Methods

3-1. Quantitative and qualitative assessment of osteomyelitis of the mandible for

prognosis prediction using diffusion-weighted magnetic resonance imaging

Subjects

This retrospective study was approved by the institutional review board (EC21-003).

This study included 61 patients with osteomyelitis of the mandible (13 men and 48

women, mean age is 68.8 years, ranging from 33 to 91 years old) who underwent MRI

from April 2017 to March 2020. Patients were diagnosed according to the clinical

symptoms (fever, malaise, swelling, local redness, pain around soft tissue, Vincent's

symptoms, and Yumikura symptoms) and typical MR imaging [T1-weighted imaging

(TIWI): low, T2-weighted imaging (T2WI): low or high, Short-tau inversion recovery

(STIR): high][6–8]. Cases that were difficult to evaluate by artifacts (n=6) and cases with

medication-related osteonecrosis of the jaw (n=23) were excluded. All patients have

followed up more than 18 months. The duration of symptoms diagnosed by oral surgeons

was investigated from electronic medical records.

Methods

MRI was performed using a 1.5-T superconductive MR unit (Intera Achieva® 1.5 T

Nova; Philips Medical Systems, Best, Netherlands) and a 5-channel phased array coil.

DWI conditions were as follows: TR/TE = 5100/70, slice thickness, 6 mm; matrix, 256×256 mm; field of view, 250×250 mm; acquisition, 3; and imaging time, 3. An ADC map was created on the MRI console.

The regions of interest were manually placed by tracing the mandibular bone marrow on the ADC map regarding the high signal region of STIR (Figure 1). The ADC values of the mandibular bone marrow were measured on the ADC map independently by two oral radiologists (S.H. and K.I., with 4 and 12 years of experience of head and neck imaging), and the average value of each value was used.

Statistical analyses

Statistical analysis was performed using Welch's t-test, dividing the cases into two groups: a group in which osteomyelitis symptoms persisted for 4 weeks or more and a group in which symptoms improved in less than 4 weeks. The intraclass correlation coefficient (ICC) was used to assess the interobserver agreement of ADC value. ICC was classified as poor (0.0-0.19), fair (0.2-0.39), moderate (0.4-0.59), good (0.6-0.79), and excellent (0.8-1.00).

Receiver operating characteristic (ROC) analysis was performed to determine the ability of ADC value to predict the prognosis of mandibular osteomyelitis. Statistical analysis was performed using the statistical package SPSS, version 28.0 (SPSS Japan,

Tokyo, Japan). A p-value of <0.05 was considered statistically significant.

3-2. Quantitative assessment of mandibular bone marrow using computed tomography

texture analysis for detect stage 0 medication-related osteonecrosis of the jaw

Subjects

This study was approved by the institutional review board (No. EC15-12-009-1) and

was conducted as a case-control study in accordance with the Helsinki Declaration. The

requirement to obtain written informed consent was waived for this retrospective study.

This study included 25 patients with stage 0 MRONJ with a history of treatment with

bisphosphonates (3 men and 22 women, mean age is 75.4 years, ranging from 48 to 88

years old) who underwent head and neck CT and MRI for suspected osteomyelitis from

April 1, 2006 to February 28, 2021 (**Figure 2**).

The mandibular bone marrow with abnormal signals (T1-weighted imaging [T1WI]:

low, T2-weighted imaging [T2WI]: low or high, short-tau inversion recovery [STIR]:

high) on MRI and no qualitative characteristic CT and oral findings of osteonecrosis

(exposed bone, sequestrum, periosteal reaction, and osteolysis) was identified as having

stage 0 MRONJ (**Figure 3**)[26,27]. Patients with bilateral MRONJ, medication-related

osteonecrosis of the maxilla, prior history of malignancy, and several artifacts on CT

images were excluded.

Methods

CT imaging was performed using a 64-multi-detector row CT scanner (Aquilion 64; Toshiba Medical Systems, Tokyo, Japan). The CT parameters were as follows: tube voltage, 120 kV; tube current, 100 mA; field of view, 240 × 240 mm; and helical pitch, 41. The protocol consisted of axial (0.50 mm) and multiplanar (3.00 mm) images.

MRI was performed using a 1.5-T superconductive MR unit (Intera Achieva 1.5T Nova; Philips Medical Systems, Best, Netherlands) with a 5-channel phased-array coil. MR images were obtained using a spin-echo sequence with the following parameters: axial T1WI (repetition time [TR], 423.9 ms; echo time [TE], 9 ms; slice thickness, 6 mm; matrix, 368 × 294; field of view [FOV], 230 × 195.5 mm), axial T2WI (TR, 4,092.8 ms; TE, 120 ms; slice thickness, 6 mm; matrix, 368 × 294; FOV, 230 × 195.5 mm), and axial STIR (TR, 2,500.0 ms; TE, 60 ms; slice thickness, 6 mm; matrix, 320 × 256; FOV, 230 × 195.5 mm). The CT and MR images were interpreted using a medical liquid crystal display monitor (RadiForce G31; Eizo Nanao, Ishikawa, Japan).

Texture features of the bone marrow of the mandible with MRONJ and the contralateral, normal mandibular bone marrow were extracted using an open-access software, namely, LIFEx[28]. Details of the texture features are described at the software

package website (https://lifexsoft.org/). The volumes of interest (VOIs) were placed by

an oral radiology specialist with 11 years of experience (**Figure 4**). Thirty-seven texture

features were extracted from each VOI.

Statistical analysis

The statistical significance of differences in 37 parameters between the bone marrow

of the mandible with MRONJ and the contralateral, normal mandibular bone marrow was

determined using the Wilcoxon rank-sum test (or paired t-test when appropriate). ROC

curve analysis was performed to identify the optimal cutoff values for selected gray-level

run length matrix (GLRLM) features (low gray-level run emphasis [LGRE], high gray-

level run emphasis [HGRE], short run low gray-level emphasis [SRLGE], short run high

gray-level emphasis [SRHGE], long run low gray-level emphasis [LRLGE], and long run

high gray-level emphasis [LRHGE]) and gray-level zone length matrix (GLZLM)

features (low gray-level zone emphasis [LGZE], high gray-level zone emphasis [HGZE],

short zone low gray-level emphasis [SZLGE], and short zone high gray-level emphasis

[SZHGE]) to detect stage 0 MRONJ on CT, and the area under the curve (AUC) was

calculated. The cutoff values were determined using the Youden index. A p-value of <0.05

was considered statistically significant. R (version 3.6.3; R Development Core Team,

Auckland, New Zealand) and SPSS software for Windows (version 21; IBM Japan Inc.,

Tokyo, Japan) were used for the analyses.

4. Results

4-1. Quantitative and qualitative assessment of osteomyelitis of the mandible for prognosis prediction using diffusion-weighted magnetic resonance imaging

Table 1 shows the characteristics and imaging findings of the patients with osteomyelitis of the mandible. The symptom-persisted group was significantly older than the symptom-improved group. There were no gender differences between the two groups (p = 0.889). There were 3 men (20.0 %) and 12 women (80.0 %) in the symptom-improved group, and 10 men (21.7 %) and 36 women (78.3 %) in the symptom-persisted group. The mean ADC value of the mandibular bone marrow in the region of mandibular osteomyelitis was $1.377 \pm 0.19 \times 10^{-3}$ mm^2/s in the symptom-persisted group and $1.198 \pm 0.11 \times 10^{-3}$ mm^2/s in the symptom-improved group, which was significantly higher in the symptom-persisted group. The interobserver agreement for the ADC value of osteomyelitis was excellent (ICC=0.881). Qualitative imaging findings, periosteal reaction and cellulitis were not significantly different between the groups (p = 0.562, 0.811). The periosteal reaction was observed in 3 patients (20.0 %) in the symptom-improved group, 6 patients (13.0 %) in the symptom-persisted group, and 9 patients (14.8 %) overall with osteomyelitis. Cellulitis was observed in 2 patients (13.3 %) in the symptom-improved group, 5 patients (10.9 %) in the symptom-persisted

16

group, and 7 patients (11.5 %) overall with osteomyelitis.

Figure 5 shows the ROC curve to determine the ability of the mean ADC value to predict the prognosis of the osteomyelitis of the mandible. A cutoff value of >1.303 × 10^{-3} mm^2/s was obtained from the ROC curve using the Youden index. If the mean ADC value of the mandibular bone marrow in the osteomyelitis of the mandible on the initial MRI shows 1.303 × 10^{-3} mm^2/s, it is predicted that the symptoms of the osteomyelitis of the mandible will last for more than 4 weeks. The AUC of the ROC curve was 0.788 (confidence interval 0.677-0.900). The sensitivity and specificity of this cutoff value were 0.933 and 0.696, respectively.

4-2. Quantitative assessment of mandibular bone marrow using computed tomography texture analysis for detect stage 0 medication-related osteonecrosis of the jaw

Table 2 shows the characteristics of patients with stage 0 MRONJ. Of the 25 patients with MRONJ, 23 were female (92%). All patients had a history of osteoporosis.

Six GLRLM features (LGRE, HGRE, SRLGE, SRHGE, LRLGE, and LRHGE) and four GLZLM features (LGZE, HGZE, SZLGE, and SZHGE) showed significant differences between normal and MRONJ-affected mandibular bone marrows (p<0.05) (**Table 3**).

Figure 6 shows the ROC curves of related texture features for detecting stage 0 MRONJ. LGRE at the cutoff value of ≤7.01e-05, HGRE at the cutoff value of ≥14906.01, SRLGE at the cutoff value of ≤6.89e-05, SRHGE at the cutoff value of ≥15024.54, LRLGE at the cutoff value of ≤8.06e-05, LRHGE at the cutoff value of ≥17323.50, LGZE at the cutoff value of ≤6.81e-05, HGZE at the cutoff value of ≥16351.96, SZLGE at the cutoff value of ≤4.84e-05, and SZHGE at the cutoff value of ≥12637.03 had AUCs of 0.7792, 0.760, 0.7848, 0.7520, 0.7456, 0.7712, 0.7832, 0.7664, 0.8112, and 0.7472, respectively. Table 4 shows the diagnostic performances of radiomics features to detect the stage 0 MRONJ. The AUCs of GLRLM features (LGRE, HGRE, SRLGE, SRHGE, and LRHGE) and GLZLM features (LGZE, HGZE, SZLGE, and SZHGE) show moderate accuracy.

5. Discussion

5-1. Quantitative and qualitative assessment of osteomyelitis of the mandible for prognosis prediction using diffusion-weighted magnetic resonance imaging

In this study, the mean ADC value of the mandibular bone marrow in the region of the osteomyelitis of the mandible was 1.377×10^{-3} mm^2/s in the symptom-persisted group and 1.198×10^{-3} mm^2/s in the symptom-improved group, which was significantly higher in the symptom-persisted group. Previous studies have shown that there are differences in ADC values in the mandibular bone marrow between normal and osteomyelitis groups[29, 30]. Normal bone marrow contains adipose tissue and stromal cells, so bacterial infection of the bone marrow is thought to increase water content in the bone marrow due to inflammatory infiltration[29]. It is thought that the persisted group had higher ADC values than the improved group due to the infiltration of inflammatory cells into the tissue. Additionally, a cutoff value of 1.303×10^{-3} mm^2/s was obtained from this study. Moreover, this cutoff value showed a high sensitivity of 0.933. If the ADC value on the initial MRI is greater than 1.303×10^{-3} mm^2/s, it is predicted that the symptoms will persist a relatively long time. Therefore, this reference value is very useful for determining clinical treatment methods.

The symptom-persisted group was significantly older than the symptom-improved

group in this study. Previous report has shown that mandibular bone marrow changes with aging[30]. It has been suggested that the trabecular structure of the mandibular cancellous bone may be lost with age. Therefore, the inflammation of the mandibular bone marrow is thought to have spread over a wide area. Additionally, the symptoms may have persisted because the immune system declines with age[31].

There was no relationship between the qualitative findings and the duration of symptoms of the osteomyelitis of the mandible from this study. This suggests that it is difficult to predict the prognosis of osteomyelitis of the mandible using computed tomography. Therefore, the reference value of ADC value obtained in this study is useful to predict the prognosis of osteomyelitis of the mandible.

5-2. Quantitative assessment of mandibular bone marrow using computed tomography texture analysis for detect stage 0 medication-related osteonecrosis of the jaw

Among 37 texture features, the bone marrow of the mandible with stage 0 MRONJ and the contralateral, normal mandibular bone marrow revealed significant differences in six GLRLM features and four GLZLM features. Moreover, these texture features exhibited a moderate diagnostic performance. Thus, texture analysis may be useful as a

new method for detecting stage 0 MRONJ using CT.

GLRLM provides the length of homogeneous runs for each grey level in thirteen different directions. LGRE or HGRE is the distribution of the low or high gray-level runs[32,33]. The bone marrow of the mandible with MRONJ had a lower LGRE and a higher HGRE than those of the bone marrow of the contralateral mandible. This indicates that the high gray-level pixels of the bone marrow of the mandible with MRONJ were frequently contiguous, and the low gray-level pixels were less contiguous. The difference in these parameters is considered to be due to osteosclerosis of the mandible with MRONJ. SRLGE or SRHGE is the distribution of the short homogeneous runs with low or high gray-levels. LRLGE or LRHGE is the distribution of the long homogeneous runs with low or high gray-levels[32,33]. The mandible with MRONJ had lower SRLGE and LRLGE, and higher SRHGE and LRHGE than those of the contralateral mandible. From these GLRLM parameters, it was evident that osteosclerosis of the mandible with MRONJ appeared as relatively linear and irregular high-density regions in the image.

The GLZLM provides information on the sizes of homogeneous zones for each gray-level in three dimensions. LGZE and HGZE indicate the distribution of low and high gray-level zones, respectively. The bone marrow of the mandible with MRONJ had

a lower LGZE and a higher HGZE than those of the contralateral mandibular bone marrow. From the difference in these parameters, it was surmised that the bone marrow of the mandible with MRONJ had lumpy high-density regions. SZLGE and SZHGE indicate the distribution of the short homogeneous zones with low and high gray-levels, respectively. Long-zone low gray-level emphasis (LZLGE) and long-zone high gray-level emphasis (LZHGE) indicate the distribution of the long homogeneous zones with low and high gray-levels, respectively. The bone marrow of the mandible with MRONJ showed a significant difference between SZLGE and SZHGE compared with the contralateral mandibular bone marrow, but no significant difference was observed between LZLGE and LZHGE. From these GLZLM parameters, it was considered that there were many relatively small lumps in the lumpy high-density regions in the bone marrow of the mandible with MRONJ.

This study has a limitation. We excluded patients with a history of treatment with antiangiogenic inhibitors. Antiangiogenic inhibitors are known to cause MRONJ. Although BRONJ and antiangiogenic inhibitor-related osteonecrosis of the jaw have been reported to have different qualitative CT findings, the differences in quantitative texture parameters obtained in this study may be applicable to the detection of antiangiogenic inhibitor-related osteonecrosis of the jaw[15]. Texture analysis of the

mandibles of patients with a history of treatment with antiangiogenic inhibitors is a

topic for future research.

6. Conclusion

This study revealed that 1) the ADC values of the mandibular bone marrow in persisted osteomyelitis and that in improved osteomyelitis, and 2) the quantitative differences between the bone marrow of the mandible with stage 0 MRONJ and the contralateral, normal mandibular bone marrow. These results suggested that quantitative assessment of osteomyelitis in the mandible using digital imaging could be very useful information in clinical situations.

7. References

1. Baur DA, Altay MA, Flores-Hidalgo A, et al. Chronic osteomyelitis of the mandible: diagnosis and management--an institution's experience over 7 years. J Oral Maxillofac Surg. 2015; 73(4): 655-665.

2. Haeffs TH, Scott CA, Campbell TH, et al. Acute and chronic suppurative osteomyelitis of the jaws: a 10-year review and assessment of treatment outcome. J Oral Maxillofac Surg. 2018; 76(12): 2551-2558.

3. Bury DC, Rogers TS, Dickman MM. Osteomyelitis: diagnosis and treatment. Am Fam Physician. 2021; 104(4): 395-402.

4. Liu D, Zhang J, Li T, et al. Chronic osteomyelitis with proliferative periostitis of the mandibular body: report of a case and review of the literature. Ann R Coll Surg Engl. 2019; 101(5): 328-332.

5. Suei Y, Taguchi A, Tanimoto K. Diagnosis and classification of mandibular osteomyelitis. Oral Surg Oral Med Oral Pathol Oral Radiol Endod. 2005; 100(2): 207-214.

6. Kaneda T, Minami M, Ozawa K, et al. Magnetic resonance imaging of osteomyelitis in the mandible. Comparative study with other radiologic modalities. Oral Surg Oral

Med Oral Pathol Oral Radiol Endod. 1995; 79(5): 634-640.

7. Kaneda T, Minami M, Ozawa K, et al. Magnetic resonance appearance of bone marrow in the mandible at different ages. Oral Surg Oral Med Oral Pathol Oral Radiol Endod. 1996; 82(2): 229-233.

8. Lee K, Kaneda T, Mori S, et al. Magnetic resonance imaging of normal and osteomyelitis in the mandible: assessment of short inversion time inversion recovery sequence. Oral Surg Oral Med Oral Pathol Oral Radiol Endod. 2003; 96(4): 499-507.

9. Ermongkonchai T, Khor R, Wada M, et al. A review of diffusion-weighted magnetic resonance imaging in head and neck cancer patients for treatment evaluation and prediction of radiation-induced xerostomia. Radiat Oncol. 2023; 18(1): 20.

10. Iwasaki T, Muraoka H. Assessment of acute osteomyelitis in the mandible using diffusion weighted MR imaging. International Journal of Oral-Medical Sciences. 2020; 18(3-4): 172-176.

11. Ogura I, Sasaki Y, Kameta A, et al. Diffusion-weighted imaging in the oral and maxillofacial region: usefulness of apparent diffusion coefficient maps and maximum intensity projection for characterization of normal structures and lesions. Pol J Radiol. 2017; 82: 571-577.

12. Ogura I, Nakahara K, Sasaki Y, et al. Diffusion-weighted magnetic resonance imaging in odontogenic keratocysts: preliminary study on usefulness of apparent diffusion coefficient maps for characterization of normal structures and lesions. Chin J Dent Res. 2019; 22(1): 51-56.

13. Otonari T, Wakoh M, Sano T, et al. Parameters for diffusion weighted magnetic resonance imaging for temporomandibular joint. The Bulletin of Tokyo Dental College. 2006; 47(1): 5-12.

14. Ruggiero SL, Dodson TB, Fantasia J, et al. American association of oral and maxillofacial surgeons position paper on medication-related osteonecrosis of the jaw--2014 update, J Oral Maxillofac Surg. 2014; 72(10): 1938-1956.

15. Querrer R, Ferrare N, Melo N, et al. Differences between bisphosphonate-related and denosumab-related osteonecrosis of the jaws: a systematic review, Support Care Cancer. 2021; 29(6): 2811-2820.

16. An CH, An SY, Choi BR, et al. Hard and soft tissue changes of osteomyelitis of the jaws on CT images, Oral Surg Oral Med Oral Pathol Oral Radiol. 2012; 114 (1): 118-126.

17. Leite AF, Ogata Fdos S, de Melo NS, et al. Imaging findings of bisphosphonate-related osteonecrosis of the jaws: a critical review of the quantitative studies, Int J

Dent, 2014; 2014: 784348.

18. Lambin P, Rios-Velazquez E, Leijenaar R, et al., Radiomics: extracting more

information from medical images using advanced feature analysis, Eur J Cancer.

2012; 48: 441-446.

19. Valdora F, Houssami N, Rossi F, et al. Rapid review: radiomics and breast cancer,

Breast Cancer Res Treat. 2018; 169: 217-229.

20. Mosquera-Lopez C, Agaian S, Velez-Hoyos A, et al. Computer-aided prostate cancer

diagnosis from digitized histopathology: a review on texture-based systems. IEEE

Rev Biomed Eng. 2015; 8: 98-113.

21. de Carvalho Alegro M1, Valotta Silva A, Yumi Bando S, et al. Texture analysis of

high-resolution MRI allows discrimination between febrile and afebrile initial

precipitating injury in mesial temporal sclerosis. Magn Reson Med. 2012; 68: 1647-

1653.

22. Jirák D, Dezortová M, Taimr P, et al. Texture analysis of human liver, J Magn Reson

Imaging. 2002; 15: 68-74.

23. Buch K, Fujita A, Li B, et al. Using texture analysis to determine human

papillomavirus status of oropharyngeal squamous cell carcinomas on CT. AJNR Am

J Neuroradiol. 2015; 36: 1343-1348.

24. Fujita A, Buch K, Li B, et al. Difference between HPV-positive and HPV-negative non-oropharyngeal head and neck cancer: texture analysis features on CT. J Comput Assist Tomogr. 2016; 40: 43-47.

25. Kuno H, Qureshi MM, Chapman MN, et al. CT texture analysis potentially predicts local failure in head and neck squamous cell carcinoma treated with chemoradiotherapy. AJNR Am J Neuroradiol. 2017; 38: 2334-2340.

26. Ruggiero SL, Fantasia J, Carlson E. Bisphosphonate-related osteonecrosis of the jaw: background and guidelines for diagnosis, staging and management. Oral Surg Oral Med Oral Pathol Oral Radiol Endod. 2006; 102: 433-441.

27. Ruggiero SL. Guidelines for the diagnosis of bisphosphonate-related osteonecrosis of the jaw (BRONJ). Clin Cases Miner Bone Metab. 2007; 4: 37-42.

28. Nioche C, Orlhac F, Boughdad S. LIFEx: A freeware for radiomic feature calculation in multimodality imaging to accelerate advances in the characterization of tumor heterogeneity. Cancer Res. 2018; 78: 4786-4789.

29. Jimenez-Boj E, Nöbauer-Huhmann I, Hanslik-Schnabel B, et al. Bone erosions and bone marrow edema as defined by magnetic resonance imaging reflect true bone marrow inflammation in rheumatoid arthritis. Arthritis Rheum. 2007; 56(4): 1118-1124.

30. Muraoka H, Ito K, Hirahara N, Okada S, Kondo T, Kaneda T. Quantitative assessment of age-related changes in the mandibular bone marrow using apparent coefficient value. Oral Radiol. 2022; 38(1): 57-62.

31. Plowden J, Renshaw-Hoelscher M, Engleman C, et al. Sambhara S. Innate immunity in aging: impact on macrophage function. Aging Cell. 2004; 3(4): 161-167.

32. Zwanenburg A, Leger S, Vallie`res M, et al. Image biomarker standardization initiative. ArXiv161207003 Cs. 2016.

33. Castellano G, Bonilha L, Li LM, Cendes F, Texture analysis of medical images, Clin Radiol. 2004; 59: 1061-1069.

8. Figures and legends

Figure 1   The region of interest (ROI) placement of the mandibular bone marrow in patients with osteomyelitis of the mandible
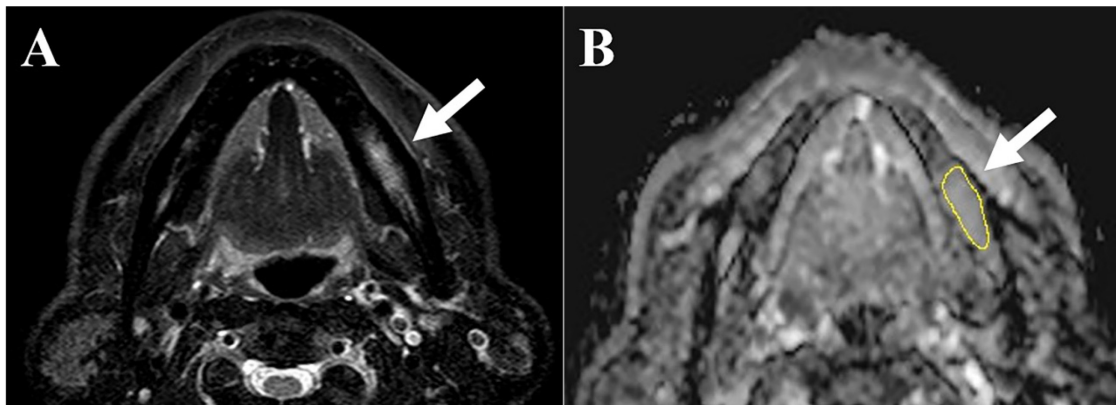
A: Axial short-tau inversion recovery image (arrow and region of interest) shows a high signal intensity in the left side of the mandibular bone marrow.

B: The apparent diffusion coefficient map (arrow and region of interest) shows a high signal intensity in the left side of the mandibular bone marrow on the region of interest.

Figure 2　Flow diagram of this study
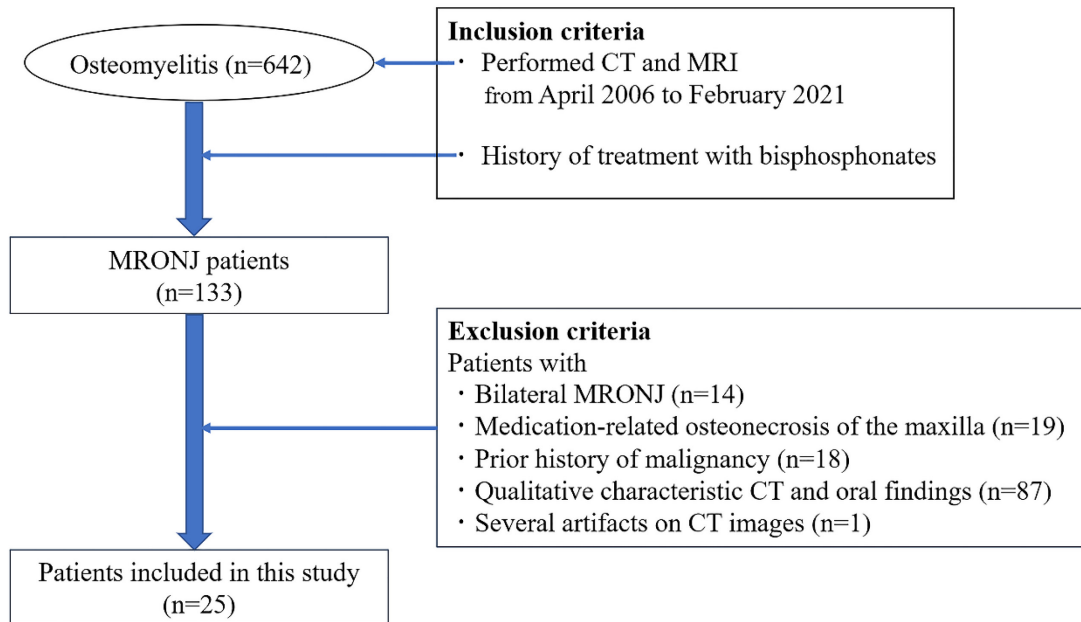
Flow diagram shows patients inclusion process for the study.

CT: computed tomography, MRI: magnetic resonance imaging, MRONJ: medication-related osteonecrosis of the jaw

Figure 3   Definition of stage 0 medication-related osteonecrosis of the jaw (MRONJ) using computed tomography (CT) and magnetic resonance imaging (MRI)
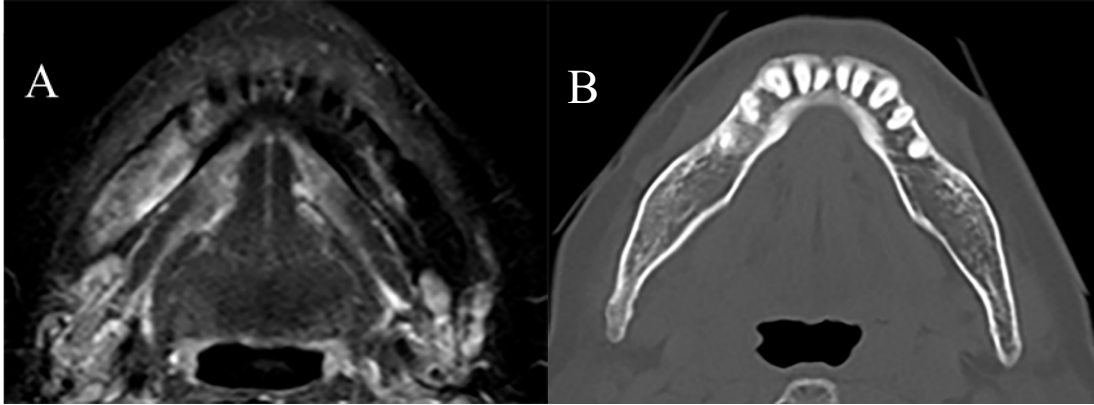
A: The CT image reveals a normal mandibular bone marrow on the left side of the mandible and stage 0 MRONJ mandibular bone marrow on the right side of the mandible.

B: The mandibular bone marrow with abnormal signals (T1WI: low, T2WI: low or high, STIR: high) on MRI were identified as stage 0 MRONJ.

Figure 4 Volume of interest (VOI) placement of mandibular bone marrow of medication-related osteonecrosis of the jaw side and opposite side on computed tomography (CT) images
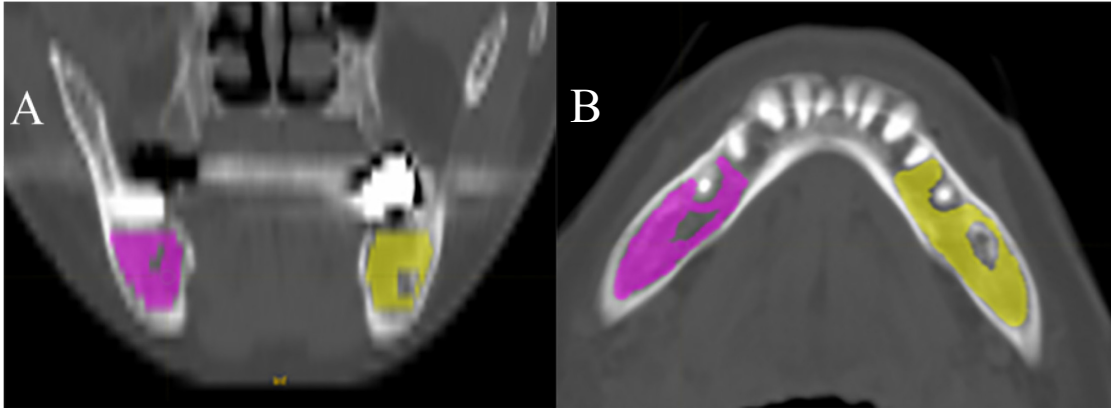
A, B: The VOIs were manually placed by tracing contours of bilateral mandibular bone marrow, excluding teeth, mandibular canal and cortical bone on CT images.

Figure 5 Receiver operating characteristic (ROC) curve analysis of apparent diffusion coefficient (ADC) value for predicting prognosis to osteomyelitis of the mandible
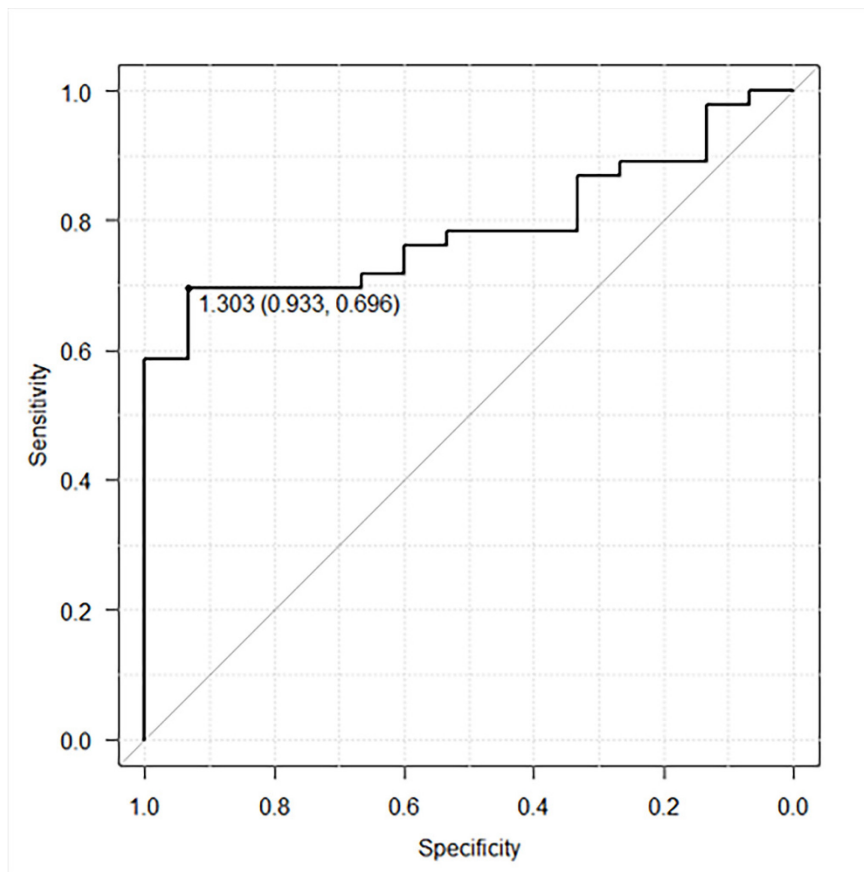
The graph shows the ROC curves of the ADC for predicting the prognosis of osteomyelitis of the mandible. ROC analysis revealed areas under the curve for maximum ADC values of 1.303. ADC apparent diffusion coefficient, The predicting prognosis to osteomyelitis of the mandible, ROC receiver operating characteristic.

Figure 6 ROC curves of related texture features for detecting stage 0 medication-related osteonecrosis of the jaw (MRONJ)
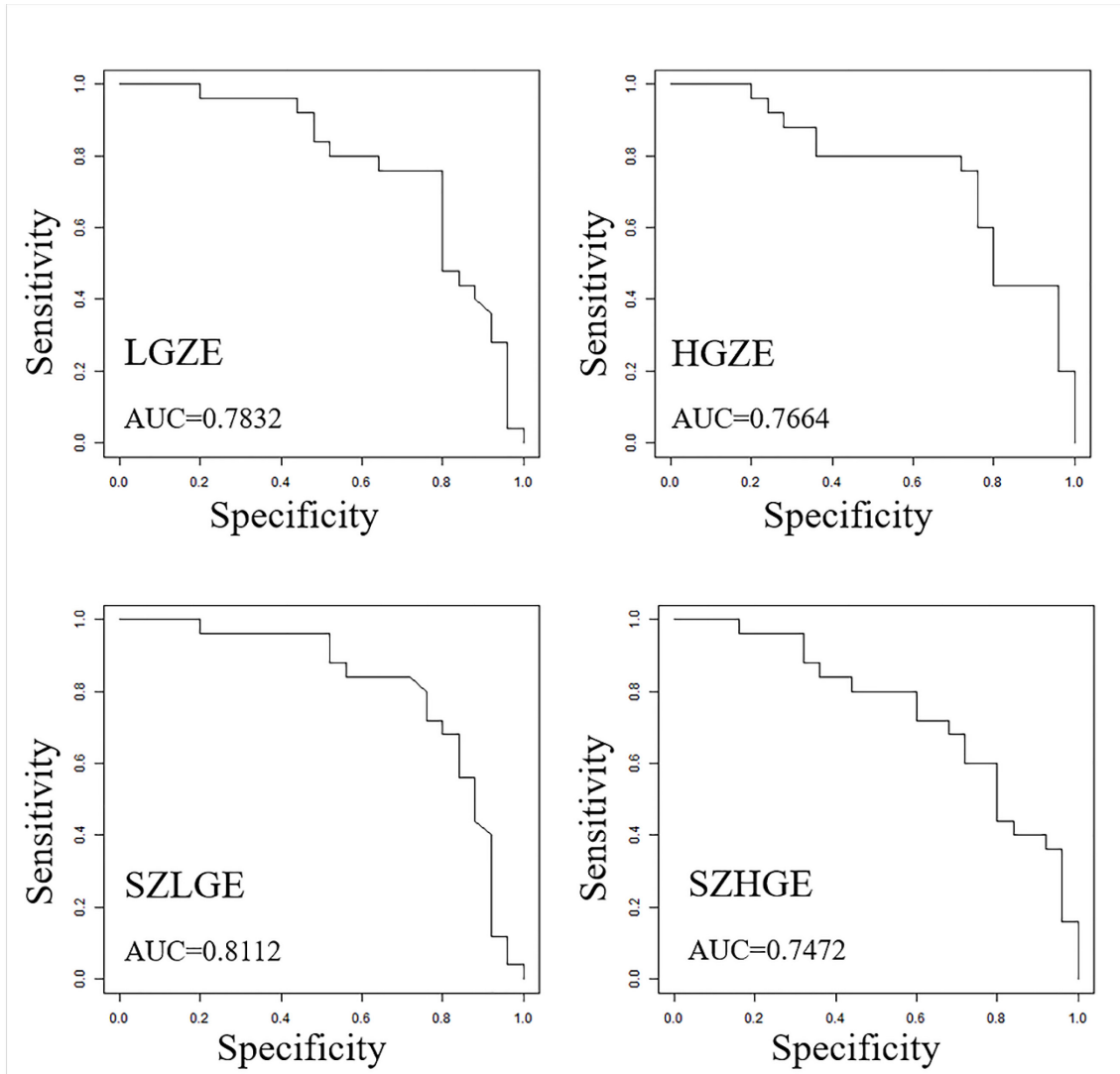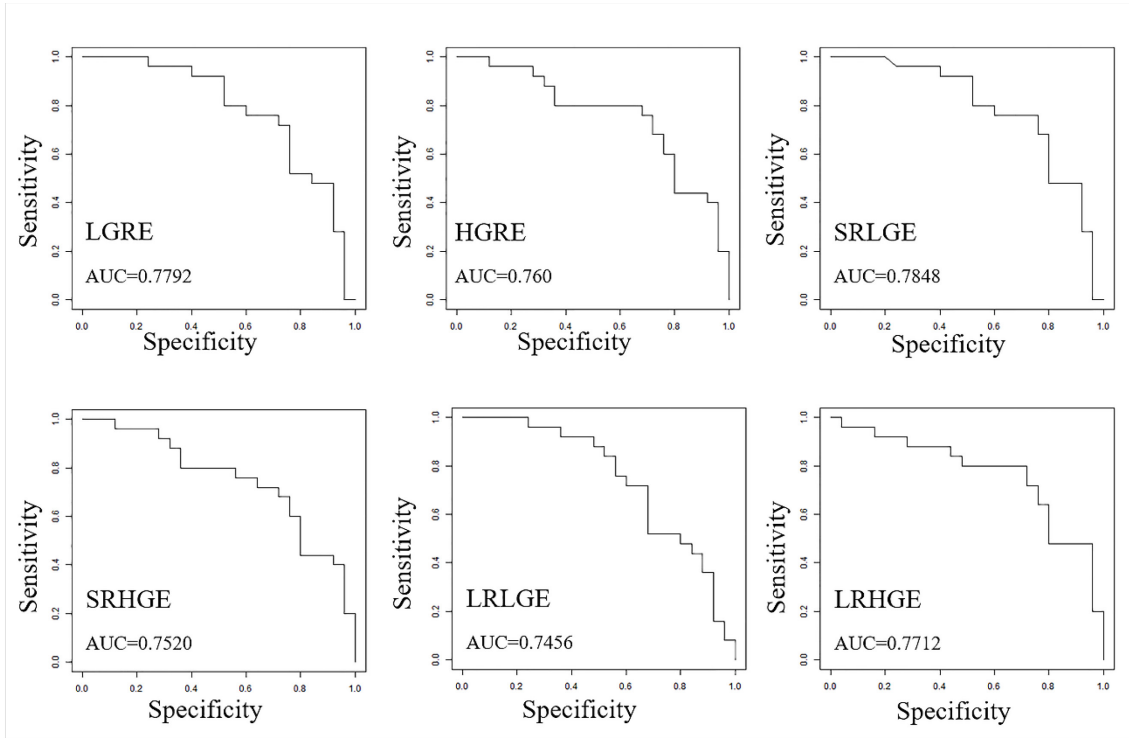
Graph shows the ROC curves of gray level run length matrix (*A*) and grey level zone length matrix (*B*) for predicting stage 0 MRONJ.

LGRE: low gray level run emphasis, HGRE: high gray level run emphasis, SRLGE: short run low gray level emphasis, SRHGE: short run high gray level emphasis, LRLGE: long run low gray level emphasis, LRHGE: long run high gray level emphasis, LGZE: low gray level zone emphasis, HGZE: high gray level zone emphasis, SZLGE: short zone low gray level emphasis, SZHGE: short zone high gray level emphasis

9. Table

Table 1   Patients' characteristics and imaging findings of the osteomyelitis of the mandible

	Improved OM (N=15)	Persisted OM (N=46)	*P value*
Age	57.07 ± 18.0	72.63 ± 14.2	6.6735e-05
Sex			
N			
male	3	10	0.889
female	12	36	
ADC value	1.198 ± 0.11	1.377 ± 0.19	0.006205375
Mean ± SD ×10^{-3}mm^2/s			
Periosteal reaction			
N			
presence	3	6	0.562
absence	12	40	
Cellulitis			
N			
presence	2	5	0.811
absence	13	41	

NOTE: OM=osteomyelitis, SD=standard deviation, N=number

Table 2   Patients' characteristics

Patient	Age	Sex M:0 F:1	MRONJ site L:0 R:1	Bisphosphonates	Medical history
1	82	1	1	Minodronic Acid Hydrate	Osteoporosis
2	74	0	1	Alendronate Sodium Hydrate	Osteoporosis
3	76	1	0	Sodium Risedronate Hydrate	Osteoporosis, RA
4	66	1	0	Alendronate Sodium Hydrate	Osteoporosis, SLE
5	65	1	1	Minodronic Acid Hydrate	Osteoporosis
6	78	1	0	Sodium Risedronate Hydrate	Osteoporosis, RA
7	48	0	1	Sodium Risedronate Hydrate	Osteoporosis
8	68	1	1	Alendronate Sodium Hydrate	Osteoporosis
9	73	1	1	Minodronic Acid Hydrate	Osteoporosis
10	72	1	1	Ibandronate Sodium Hydrate	Osteoporosis
11	81	1	1	Ibandronate Sodium Hydrate	Osteoporosis
12	75	1	0	Minodronic Acid Hydrate	Osteoporosis
13	82	1	0	Sodium Risedronate Hydrate	Osteoporosis
14	71	0	1	Alendronate Sodium Hydrate	Osteoporosis
15	80	1	0	Minodronic Acid Hydrate	Osteoporosis
16	85	1	1	Minodronic Acid Hydrate	Osteoporosis
17	88	1	0	Alendronate Sodium Hydrate	Osteoporosis
18	67	1	1	Alendronate Sodium Hydrate	Osteoporosis
19	74	1	0	Minodronic Acid Hydrate	Osteoporosis
20	81	1	1	Minodronic Acid Hydrate	Osteoporosis
21	82	1	0	Alendronate Sodium Hydrate	Osteoporosis
22	83	1	1	Minodronic Acid Hydrate	Osteoporosis
23	70	1	1	Minodronic Acid Hydrate	Osteoporosis, DM
24	82	1	1	Ibandronate Sodium Hydrate	Osteoporosis
25	84	1	0	Minodronic Acid Hydrate	Osteoporosis

NOTE: RA: rheumatoid arthritis, SLE: systemic lupus erythematosus, DM: diabetes

mellitus, M: Male, F: Female, L: Left, R: Right,

Table 3 Radiomics features differentiating between stage 0 MRONJ site and non-MRONJ site using Wilcoxon rank sum test and paired t-test

Texture features	Stage0 MRONJ site	Non-MRONJ site	Wilcoxon rank-sum test	Paired t-test
			p-value	
Histogram				
Skewness	2.83±1.01	3.25±0.80	0.082	
Kurtosis	11.65±7.10	14.02±6.60	0.090	
Entropy-log10	1.87±0.15	1.79±0.14	0.133	
Entropy-log2	6.20±0.50	5.93±0.46	0.133	
Energy	0.018±0.0076	0.022±0.0083	0.128	
GLCM				
Homogeneity	0.19±0.050	0.21±0.039		0.082
Energy	0.0012±0.00086	0.0014±0.00089	0.090	
Contrast	393.49±260.33	274.32±158.92	0.128	
Correlation	0.61±0.14	0.54±0.16	0.190	
Entropy-log10	3.16±0.22	3.05±0.19	0.093	
Entropy-log2	10.50±0.73	10.13±0.63	0.093	
Dissimilarity	13.20±4.90	11.08±3.29	0.138	
GLRLM				
SRE	0.97±0.01	0.97±0.0088	0.148	
LRE	1.13±0.068	1.14±0.068	0.190	
LGRE	6.22e-05±1.34e-05	7.5e-05±1.03e-05		9.62e-06*
HGRE	19007.39±5000.42	14985.7±2805.068	0.0016*	
SRLGE	6.03e-05±1.25e-05	7.27e-05±9.55e-06		7.28e-06*
SRHGE	18613.79±5023.18	14631.79±2845.00	0.0022*	
LRLGE	7.16e-05±1.85e-05	8.75e-05±1.58e-05		3.87e-05*
LRHGE	20910.89±4860.64	16762.43±2550.76	0.0010*	
GLNU	60.31±38.30	64.22±31.48	0.377	
RLNU	3243.33±1669.31	2932.68±1515.88	0.421	
RP	0.97±0.015	0.96±0.013	0.154	
NGLDM				
Coarseness	0.0031±0.0012	0.0032±0.0012		0.35
Contrast	0.70±0.46	0.47±0.22	0.105	
Busyness	0.028±0.014	0.029±0.013	0.621	
GLZLM				
SZE	0.79±0.048	0.77±0.042	0.105	
LZE	6.84±9.74	6.64±5.51	0.177	
LGZE	5.91e-05±1.2e-05	7.14e-05±9.75e-06		4.79e-06*
HGZE	19913.9±4855.47	15861.55±2911.22	0.0012*	
SZLGE	4.49e-05±7.27e-06	5.29e-05±5.52e-06		1.62e-06*
SZHGE	16271.41±4657.82	12704.43±2961.58	0.0027*	
LZLGE	0.00054±0.00087	0.00058±0.00053	0.070	
LZHGE	96661.15±108479.3	81554.94±57094.58	0.884	
GLNU	33.37±14.02	34.20±13.89	0.99	

ZLNU	1327.57±645.94	1084.88±466.96	0.138
ZP	0.656±0.10	0.62±0.090	0.133

NOTE: MRONJ=medication-related osteonecrosis of the jaw, GLCM=gray level co-occurrence matrix, GLRLM=gray level run length matrix, NGLDM=neighborhood grey level different matrix, GLZLM=grey level zone length matrix, SRE=short run emphasis, LRE=long run emphasis, LGRE=low gray level run emphasis, HGRE=high gray level run emphasis, SRLGE=short run low gray level emphasis, SRHGE=short run high gray level emphasis, LRLGE=long run low gray level emphasis, LRHGE=long run high gray level emphasis, GLNU=gray level non uniformity, RLNU=run length non uniformity, RP=run percentage, SZE=short zone emphasis, LZE=long zone emphasis, LGZE=low gray level zone emphasis, HGZE=high gray level zone emphasis, SZLGE=short zone low gray level emphasis, SZHGE=short zone high gray level emphasis, LZLGE=long zone low gray level emphasis, LZHGE=long zone high gray level emphasis, ZLNU=zone length non uniformity, ZP=zone percentage, *p<0.01

Table 4 Diagnostic performances of texture parameters to predict stage0 MRONJ

	Threshold criterion	TP	FP	FN	TN	Sensitivity (%)	Specificity (%)	Accuracy	AUC
GLRLM									
LGRE	≤7.01e-05	19	7	6	18	76.0	72.0	0.740	0.7792
HGRE	≥14906.01	19	7	6	18	76.0	72.0	0.740	0.760
SRLGE	≤6.89e-05	19	6	6	19	76.0	76.0	0.760	0.7848
SRHGE	≥15024.54	18	7	7	18	72.0	72.0	0.720	0.7520
LRLGE	≤8.06e-05	18	8	7	17	72.0	68.0	0.700	0.7456
LRHGE	≥17323.50	20	7	5	18	80.0	72.0	0.760	0.7712
GLZLM									
LGZE	≤6.81e-05	19	5	6	20	76.0	80.0	0.780	0.7832
HGZE	≥16351.96	19	6	6	19	76.0	76.0	0.760	0.7664
SZLGE	≤4.84e-05	20	6	5	19	80.0	76.0	0.780	0.8112
SZHGE	≥12637.03	18	8	7	17	72.0	68.0	0.700	0.7472

NOTE: TP=true positive, FP=false positive, FN=false negative, TN=true negative,

AUC=area under the curve, GLCM=gray level co-occurrence matrix, GLRLM=gray

level run length matrix, GLZLM=grey level zone length matrix, LGRE=low gray level

run emphasis, HGRE=high gray level run emphasis, SRLGE=short run low gray level

emphasis, SRHGE=short run high gray level emphasis, LRLGE=long run low gray level

emphasis, LRHGE=long run high gray level emphasis, SZE=short zone emphasis,

LGZE=low gray level zone emphasis, HGZE=high gray level zone emphasis,

SZLGE=short zone low gray level emphasis, SZHGE=short zone high gray level

emphasis, ZP=zone percentage